JOURNAL OF MATERIALS SCIENCE **34** (1999) 6115–6119

Electrical properties of $(Ba,Sr)TiO_3$ on $(Sr,Ca)RuO_3$ electrode

SEUNG YOUNG SON, BOUM SEOCK KIM, SE HOON OH, DUCK KYUN CHOI
Department of Inorganic Materials Engineering, Hanyang University, Seoul 133-791, Korea
E-mail: duck@email.hanyang.ac.kr

CHA YOUNG YOO, SANG IN LEE
Semiconductor R&D Center, Samsung Electronics Co., San No. 24, Nongseo-Lee, Kiheung-Eup, Yongin-Gun, Kyungki-Do 449-900, Korea

Z. R. DAI, FUMIO S. OHUCHI
Department of Material Science and Engineering, University of Washington, Seattle, WA 19890, USA

A perovskite $(Sr,Ca)RuO_3$ [SCR] electrode has been explored in order to utilize its advantages in structural match with $(Ba,Sr)TiO_3$ [BST] films, which may enhance the electrical properties of BST films. The SCR electrode led to the leakage current density ($10^{-7}A/cm^2$) of BST films an order lower than that on RuO_2. The leakage current was not sensitive to the composition of the SCR electrodes, while the dielectric constant of the BST thin film capacitor ranged from 160 to 280 depending on the Sr/Ca ratio in SCR electrodes. The BST/SCR (Sr/Ca = 7/3) system resulted in a 5-nm thick interfacial layer. Furthermore, the interfacial layer turned out to be partially crystallized according to the lattice image taken by an HRTEM. It is believed that such enhancement in electrical properties of BST films could be induced by the improvement of interfacial characteristics through structural matching.

1. Introduction

Post-Gbit dynamic random access memory (DRAM) capacitors which utilize ferroelectric materials have been studied extensively for many years. In order to realize a simple capacitor structure with a high charge density, preparation of ferroelectric material is known to be a key for ULSI device applications. $(Ba_xSr_{1-x})TiO_3$ [BST] is an attractive capacitor material for DRAMs, since it has chemical stability and good dielectric properties compared to the other ferroelectric materials such as $Pb(Zr_xTi_{1-x})O_3$ and $BaTiO_3$ [1–3]. To date, Pt has been the most widely used electrode for dielectric layers. However, it requires a multi-layer (Pt/TiN/Ti/Si) structure which is complicated to process and it exhibits poor properties in fatigue and etching. On the other hand, RuO_2 conductive oxide material has been explored with the expectation that it could overcome such problems [4–7]. It has been reported that the RuO_2 electrode acts as an effective diffusion barrier against oxygen and has a relatively low resistivity applicable for the electrode. Also, RuO_2 can be easily etched anisotropically by a gas mixture of CF_4 and H_2. And, it is quite physically and chemically stable at a high deposition temperature [8–10]. But, the practical use of RuO_2 is still limited by such the problems as a relatively high leakage current associated with a low barrier height and a degradation of the dielectric constant caused by the chemical and the structural incompatibility with the BST [11, 12].

Thus, it is very encouraging to investigate the perovskite structured $(Sr,Ca)RuO_3$ [SCR] conductive oxide electrode under the assumption that the proper modification in structure and composition could enhance the electrical properties. Noting that the lattice parameter of $(Ba_{0.5}Sr_{0.5})TiO_3$ is 3.92 Å, it is possible for SCR to match perfectly with BST, since the lattice parameter of SCR can be tuned from 3.83 to 3.93 Å, depending on the Sr/Ca ratio [13]. In addition, SCR could effectively suppress the interdiffusion between BST and SCR layers due to the common Sr. In this study, SCR films with various Sr/Ca ratios were prepared by adding Sr and Ca to RuO_2. Also, the effect of the Sr/Ca ratios on the dielectric constant and the leakage current of ferroelectric thin films was investigated.

2. Experimental procedure

A $(Sr,Ca)RuO_3$ sputtering target was prepared by uniaxially pressing the mixture of RuO_2, SrO and CaO calcined at 1000 °C. SCR films were deposited on a P-type (100) Si wafer by an RF magnetron sputter using the targets with various Sr/Ca ratios, Sr/Ca = 7/3, 5/5, 9/1, 10/0. BST films were also deposited by an RF magnetron sputtering system using a cold pressed target of (Ba + Sr)/Ti = 1.025 considering the sputtering yield. Then, Al top electrodes were deposited by a thermal evaporation method through a metal hard mask to investigate the electrical properties

of Al/BST/SCR thin film capacitors. The deposition conditions for SCR and BST films are summarized in Table I. An X-ray diffraction was performed to determine the crystalline phases and to calculate the lattice parameter of SCR and BST films. The surface morphology of specimens was observed by a Scanning Electron Microscope (SEM). An AES analysis was carried out to profile the elemental distribution at the interface in BST/SCR thin films. More careful investigation of the interface between the ferroelectric film and the bottom electrode was done by a High Resolution Transmission Electron Microscopy (HRTEM). The leakage current characteristics were analyzed by an HP4145B semiconductor parameter analyzer. The dielectric constant was calculated from the capacitance measured by an HP4280A 1 MHz C meter/CV plotter.

TABLE I Deposition conditions of SCR and BST films

	$(Sr,Ca)RuO_3$	$(Ba,Sr)TiO_3$
O_2/Ar ratio	1/9	5/5
Substrate temperature (°C)	500	550
Working pressure (mTorr)	10	10
Target Composition	Sr/Ca = 5/5, 7/3, 9/1, 10/0	Ba/Sr = 5/5
Target Size (inch)	3	3
RF-Power (W)	130	130
Thickness (nm)	300	200

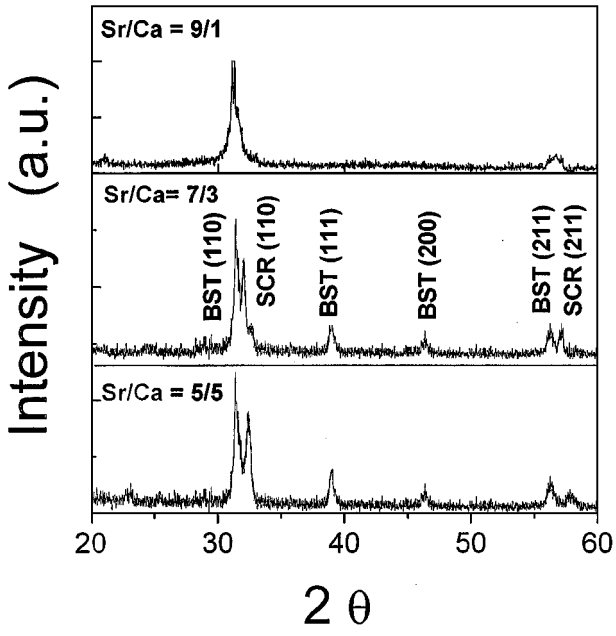

Figure 1 XRD patterns of BST/SCR with various Sr/Ca ratios in SCR electrodes.

3. Results and discussion

X-ray diffraction patterns of $(Ba,Sr)TiO_3$ films deposited on the $(Sr,Ca)RuO_3$ bottom electrode with various Sr/Ca ratios are shown in Fig. 1. The thickness of $(Ba,Sr)TiO_3$ and $(Sr,Ca)RuO_3$ film are 200 and 300 nm, respectively. Regardless of the composition of the bottom electrode, all the $(Ba,Sr)TiO_3$ films show (110) preferred orientation following the orientation of SCR which has the same cubic perovskite structure as BST films. As the Sr/Ca ratio in SCR increases and, therefore, the lattice constant of SCR approaches that of BST (3.92 Å), (111) and (200) diffraction peaks from

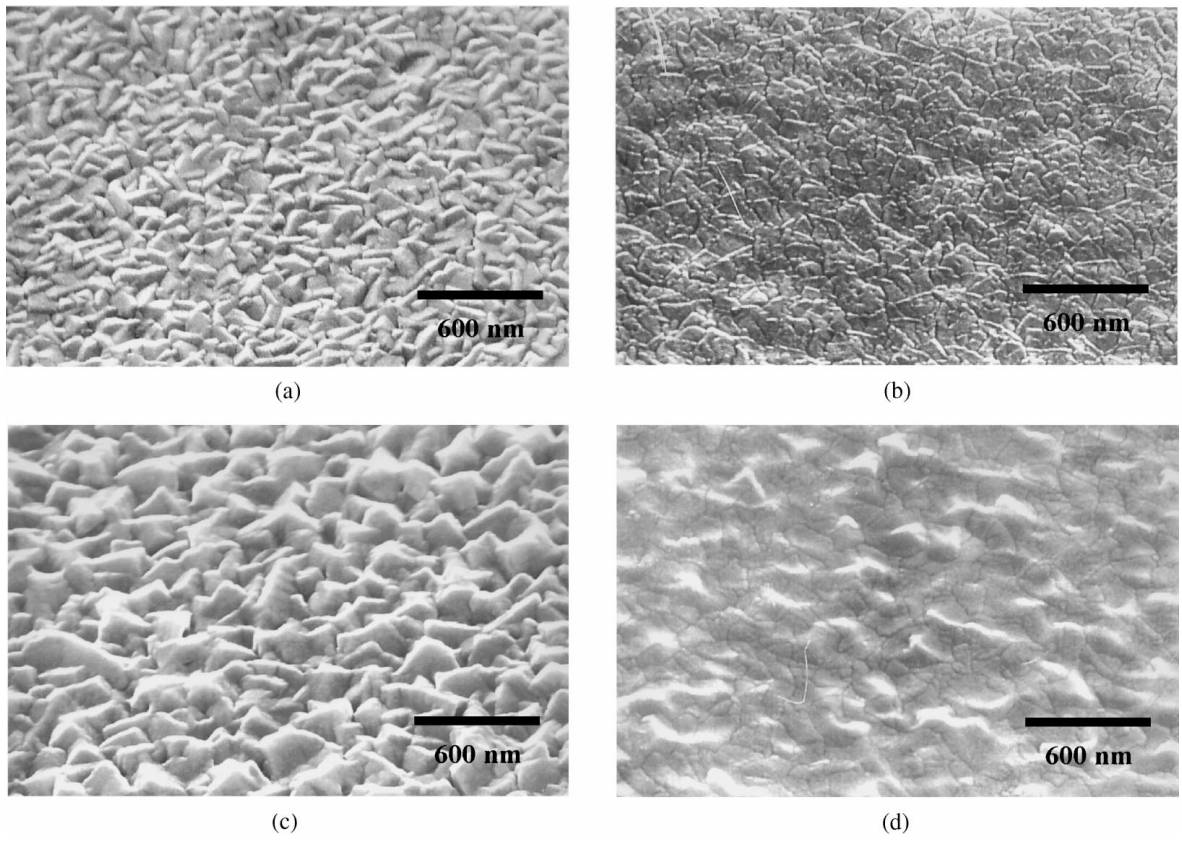

Figure 2 The surface morphologies of SCR electrodes and BST/SCR films with different Sr/Ca ratios in SCR electrodes. (a) SCR (Sr/Ca = 7/3), (b) BST/SCR (Sr/Ca = 7/3), (c) SCR (Sr/Ca = 5/5) and (d) BST/SCR (Sr/Ca = 5/5).

BST disappear gradually. Since the lattice parameter of SCR calculated from the peak at the high Bragg angle changes from 3.87 to 3.93 Å as the Sr/Ca ratio varies from 5/5 to 9/1, the lattice parameter of SCR can be perfectly tuned to that of BST (3.92 Å) by a judicious selection of the composition. The successful lattice matching between SCR and BST was observed when the Sr/Ca ratio was 9/1 and the split of the Bragg angle between BST(110) and SCR(110) was not shown.

The surface morphologies of the SCR and BST/SCR films are shown in Fig. 2a–d, respectively. The SEM images of SCR electrodes show that the SCR (Sr/Ca = 5/5) electrode has a rougher surface and larger grains than SCR (Sr/Ca = 7/3). It turned out that the surface morphology of BST films is closely linked to that of the SCR substrate. The grain size of the BST film deposited on SCR (Sr/Ca = 5/5) electrode is approximately 60–70 nm while that of BST/SCR (Sr/Ca = 7/3) is about 40–50 nm. Such grain size differences in the BST/SCR systems with various Sr/Ca ratios in electrodes are reflected in the electrical properties.

Using Rutherford Back Scattering (RBS), SCR films deposited with the targets having Sr/Ca ratios of 5/5, 7/3 and 9/1 were characterized and the practical compositions of the resulted films turned out to be $(Sr_{0.47}Ca_{0.53})RuO_3$, $(Sr_{0.61}Ca_{0.39})RuO_3$ and $(Sr_{0.90}Ca_{0.10})RuO_3$, respectively. The slight difference in compositions between the targets and the resulting films is from the sputtering yield difference between the elements. In our results hereafter, all the properties will be compared as a function of Sr/Ca ratios in targets instead of a real composition of films.

The leakage current properties of BST on the various SCR electrodes are shown in Fig. 3. Irrespective of the SCR compositions, the leakage current of BST films increases slowly with the applied voltage. It is verified from the I-V characteristic that the current through BST film capacitor is electrode-limited, because the shape of curve for negative bias is different from that for positive bias. Since Al has a relatively low work function, the potential barrier height between Al and BST is small at contact. Such an effect will lead to the absence of the flat region in the I-V curve when the negative bias is applied to the top electrode. On the contrary, when the positive bias was applied to the top electrode, the flat region appeared because of a relatively high potential barrier between SCR and BST.

The leakage current densities of BST films on the various electrodes at DRAM operation voltage of 0.1 MV/cm are shown in Fig. 4. The leakage current density of BST film on the SCR electrode is in the range of 10^{-7}A/cm^2, which is compatible to the specification

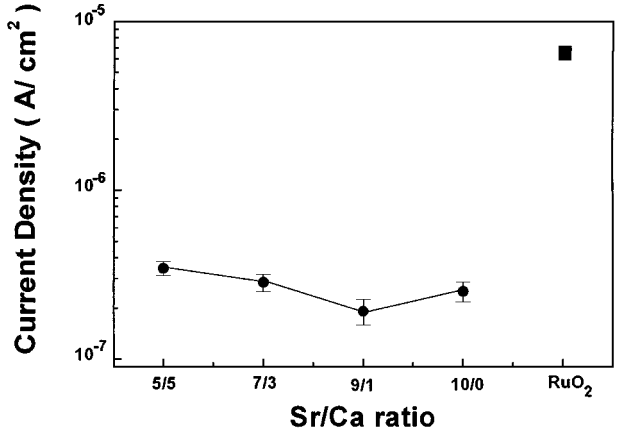

Figure 4 Variation in leakage current density of BST films as a function of Sr/Ca ratios in SCR electrodes (●) and the RuO_2 (■) electrode at 0.1 MV.

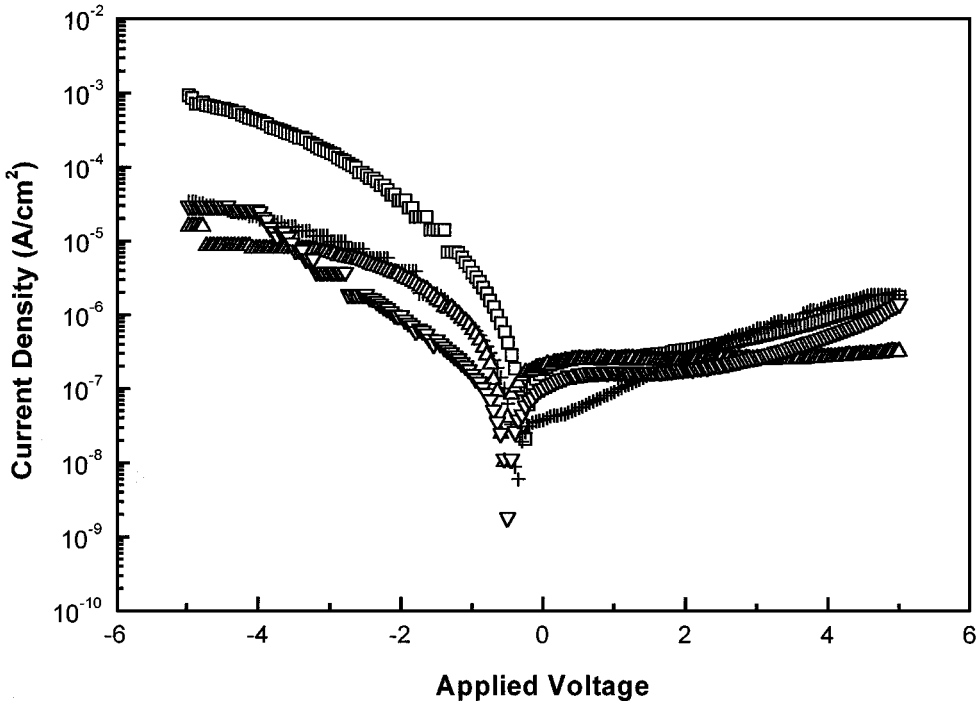

Figure 3 I-V characteristics of BST/SCR with various electrode compositions. The Sr/Ca ratios of SCR are 5/5(□), 7/3(+), 9/1(▽) and 10/0(△).

in practical devices. This value is about one order of magnitude lower than the value reported in the case of the BST/RuO_2 system (6×10^{-5}A/cm^2) [14]. For a system having different structures between the dielectric layer and an electrode like a BST/RuO_2 system, an amorphous interfacial layer is likely to form, which has the possibility of blocking the path of the leakage current. However, at the same time, the structural mismatch provides a better chance to generate defects, which could act as sources for leakage current. Presumably the latter effect overwhelms the former effect in the BST/RuO_2 system. Indeed, Izuha *et al*. [15] reported in their system of (Ba,Sr)TiO_3/$SrRuO_3$ which consists of an identical structure, that the minimization of the lattice distortion at the interface and the ion vacancy due to structural match led to the reduction in leakage current.

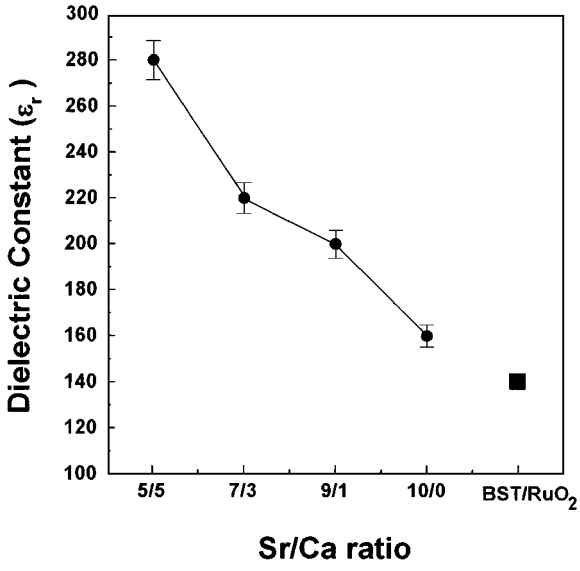

Figure 5 Dielectric constants of BST films as a function of Sr/Ca ratios in SCR electrodes (●) and the RuO_2 (■) electrode.

Fig. 5 illustrates the dielectric constant of BST films as a function of the Sr/Ca ratio in the SCR target. And two features can be pointed out. One of the results is that the dielectric constants of BST films deposited on SCR are higher than those on RuO_2 which range from 130 to 160 [13]. It is well known that the undesired interfacial layer has a low dielectric constant and behaves as a series capacitor. Also, the overall dielectric constant, which is calculated from the total capacitance, depends on the relative thickness of the low dielectric phase. The thickness of the interfacial layer in the BST/SCR system is believed to be thinner than that in the BST/RuO_2 system, because SCR is the same as BST in terms of structure. Hence, the dielectric constant of BST/SCR is higher than that of BST/RuO_2. The reason the BST/Pt system shows a high dielectric constant is associated with the grain size of BST grown on Pt [16]. Fig. 5 also shows that the dielectric constants of BST films are dependent on the composition of SCR films. However, leakage current properties of BST films are not very sensitive to the composition of SCR films. It is believed that the increment of the dielectric constant as the Sr/Ca ratio approaches to 5/5 is not only because the

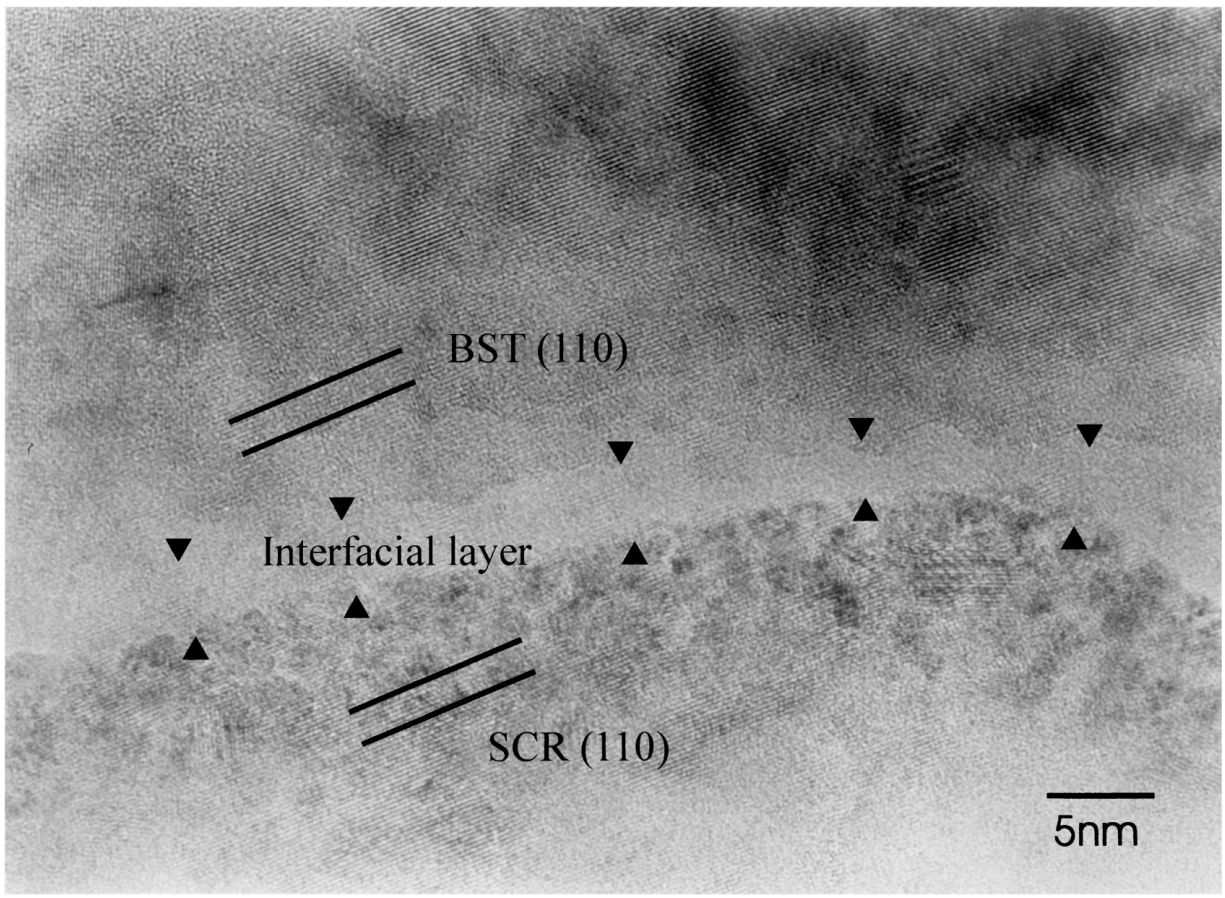

Figure 6 HRTEM image of the interface between BST film and the SCR (Sr/Ca = 7/3) electrode.

BST/SCR (Sr/Ca = 5/5) system results in larger grains than BST/SCR (Sr/Ca = 7/3) system but also because this composition in SCR electrode can help to keep the stoichiometry in BST film by suppressing the driving force for the diffusion between elements.

In order to visualize the advantage of structural matching, the interface between BST and SCR was examined by HRTEM (Fig. 6). It was found that BST films grew to (110) orientation following (110) lattice fringe of the bottom electrode. This result corresponds to the previous XRD result in that the orientation of dielectric films was largely affected by preferred orientation of the bottom electrode. The continuous lattice fringes at some portion of the interface seen from the HRTEM image indicate that two films can even form a partially crystallized interface. It reveals a 5-nm thick interfacial layer in BST/SCR. Consequently, this improvement in interfacial layer thickness results from the structural similarity obtained by applying a perovskite oxide electrode.

4. Conclusions

The electrical properties of (Ba,Sr)TiO_3 thin films were investigated in terms of the microstructure and composition of the (Sr,Ca)RuO_3 bottom electrode. HRTEM image has proven the structural advantage of the perovskite electrode on the BST dielectric film. It shows a partially crystallized thin interfacial layer between BST and SCR. Such improvement in interfacial properties led to the enhancement in electrical properties of BST films. The leakage current of BST film on SCR electrodes is about one order less than that on RuO_2 films processed under the same laboratory conditions. This is thought to be from the mechanical stability at the interface and the decrease of defects induced by a structural match. Also, the improvement in property of low dielectric layer at the interface by adopting the electrode with the same structure and similar composition, resulted in the increase in the dielectric constant of BST/SCR compared to BST/RuO_2.

Acknowledgement

This work was supported by the Korea Science and Engineering Foundation (KOSEF) and the National Science Foundation (NSF).

References

1. J. F. SCOTT, M. AZUMA, E. FUJII, T. OTSUKI, G. KANO, M. C. SCOTT, C. A. PAZDE ARANJO, L. D. McMILLAN and T. ROBERT, *IEEE* (1992) 356–359.
2. K. ABE and S. KOMATSU, *J. Appl. Phys.* **77** (1995) 6461.
3. S. H. PAEK, J. H. WON, K. S. LEE, J. S. CHOI and C. S. PARK, *Jpn. J. Appl. Phys.* **35** (1996) 5757–5762.
4. S. K. HONG, H. J. KIM and H. G. YANG, *J. Appl. Phys.* **80**(2) (1996) 822–826.
5. K. TAKEMURA, T. SAKUMA and Y. MIYASAKA, *Appl. Phys. Lett.* **64**(22) (1994) 2967–2969.
6. WEI PAN and SESHU B. DESU, *J. Mat. Res.* **9**(11) (1994).
7. H. N. AL-SHAREEF, K. D. FIFFORD, P. D. HREN, S. H. ROU, O. AUCIELLO and A. I. KINGON, 4th International Symposium on Integrated Ferroelectrics **2** (1992) 181–196.
8. D. P. VIJALY and S. B. DESU, *J. Electrochem. Soc.* **140**(9) (1993) 2640–2645.
9. H. MAIWA, N. ICHINOSE and K. OKAZAKI, *Jpn, J. Appl. Phys.* Part 1, **33**(9B) (1994) 5223–5226.
10. L. KRUSIN-ELBAUM, M. WITTNER and D. S. YEE, *Appl. Phys. Lett.* **50**(26) (1987) 1879–1881.
11. P. D. HREN, S. H. ROU, H. N. AL-SHARAEEF, M. S. AMEEN, O. AUCIELLO and A. I. KINGON, *Integrated Ferroelectrics* **2** (1992) 311–325.
12. S. D. BERNSTEIN, T. Y. WONG, Y. KISLER and R. W. TUSTISON, *J. Mater. Res.* **8**(1) (1993) 12–13.
13. C. B. EOM, R. J. CAVA, R. M. FLEMING, JULIA M. PHILLIPS, R. B. VAN DORVER, J. H. MARSHALL, J. W. P. HSU, J. J. KRAJEWSKI and W. F. PECK, JR., *Science* **258** (1992) 1766.
14. SU-HYON PAEK, KONG-SOO LEE, JIN-YONG SEONG, DUCK-KYUN CHOI, BOUM-SEOCK KIM and CHI-SUN PARK, *J. Vac. Sci. Technol. A* **16**(4) (1998) pp. 2448–2453.
15. MITSUAKI IZUHA, KAZUHIDE ABE and NOBURU FUKUSHIMA, *Jpn. J. Appl. Phys.* **36** (1997) 5866–5869.
16. TSUYOSHI HORIKAWA, NOBORU MIKAMI, TETSURO MAKITA, JUNJI TANIMURA, MASAYUKI KATAOKA, KAZUNAO SATO and MASAHIRO NUNOSHITA, *Jpn. J. Appl. Phys.* **32** (1993) 4126–4130.

Received 3 April 1998
and accepted 4 May 1999